Chemical Engineering Journal 463 (2023) 142474

Contents lists available at ScienceDirect

Chemical Engineering Journal

journal homepage: www.elsevier.com/locate/cej

Short communication

Sintering-free catalytic ammonia cracking by vertically standing 2D porous framework supported Ru nanocatalysts

Seok-Jin Kim [a,b,c], Thien Si Nguyen [a,b], Javeed Mahmood [a,b,*], Cafer T. Yavuz [a,b,c,*]

[a] Oxide & Organic Nanomaterials for Energy & Environment (ONE) Laboratory, Physical Science & Engineering (PSE), King Abdullah University of Science and Technology (KAUST), Thuwal 23955, Saudi Arabia
[b] Advanced Membranes & Porous Materials (AMPM) Center, Physical Science & Engineering (PSE), King Abdullah University of Science and Technology (KAUST), Thuwal 23955, Saudi Arabia
[c] KAUST Catalysis Center (KCC), Physical Science & Engineering (PSE), King Abdullah University of Science and Technology (KAUST), Thuwal 23955, Saudi Arabia

ARTICLE INFO

Keywords:
Ruthenium nanocatalysts
Porous phenazine frameworks
Thermal decomposition
Layered materials
Aggregation prevention
Green hydrogen fuel

ABSTRACT

Catalytic ammonia decomposition enables ammonia to be a hydrogen gas carrier for a carbon-free fuel economy. The challenge is to obtain high conversion yields and rates at low temperatures for a prolonged time. A promising approach is to engineer a catalyst support to minimize deleterious effects like sintering. Here, we compared a conventional 2D planar porous framework support with a vertically standing 2D structure to ascertain the effects of support geometry on the catalytic performance. The catalysts were made by loading ruthenium (Ru) nanoparticles onto the structures, and the catalytic activities were monitored by varying the ammonia (NH_3) feeding rate and reaction temperature. Unlike the planar version, the vertically standing 2D support prevented nanoparticle aggregation, retained the original nanoparticle size, and showed an excellent hydrogen production rate (95.17 mmol g_{Ru}^{-1} min^{-1}) at a high flow rate of 32,000 mL g_{cat}^{-1} h^{-1} at a temperature of 450 °C.

1. Introduction

In heterogeneous catalysis, targeted design of a catalyst support could foster effective use of the catalytic sites and maximize the catalytic activity [1–4]. Porous supports with large surface areas are widely used to anchor active metal catalysts [5,6]. Fabricating catalyst support *via* a bottom-up strategy using polymerization reactions can be a simple way to achieve desired pore sizes and anchoring sites [5,7].

For catalyst stability, it is widely believed that designing catalyst supports with polar surfaces is beneficial for maintaining tight interactions with metal particles. Therefore, studies focused on catalyst supports with a heteroatomic layout [8,9]. In particular, nitrogen (N)-doped carbon structures or defects feature localized electrons that function as metal anchoring sites [1]. These carbon nitride structures have been studied as support platforms to confine nanoparticles for efficient catalysis [5]. Monomers with N-containing functional groups such as phenazine, triazine, phthalocyanine, benzimidazole, isoindolone, and anthrazoline, could, therefore, be used to construct two-dimension (2D) or three-dimension (3D) organic frameworks as catalyst supports [10–16].

2D catalyst supports often have large surface areas relative to their masses [1]. The 2D materials with fused aromatic systems can be particularly useful for metal-anchoring on their surfaces. Their predominant sp^2 hybridization [13] makes them excellent catalyst supports with better thermal stability than conventional structure formed by carbonization of the linear polymer [17,18]. The catalytic activity, however, generally decreases over time due to the catalyst migration across the support's unobstructed surface during a high temperature catalytic reaction [19]. In addition, the interlayer interactions between the 2D layers inevitably cause surface area losses due to strong π-π stacking [20].

To lessen interlayer interactions while building a 2D polymer with a very high surface area, vertically standing 2D structures from monomers with perpendicular extensions proved effective by deforming the C_2 symmetry in the final, fused aromatic framework [20,21]. 2D extended ladder polymers, in particular, often have an intrinsic microporous structure and provide the advantage of efficient processing of a large amount of gas in separation applications because of their excellent permittivity [22]. In addition, a fully conjugated ladder-type backbone possesses extraordinary thermal and chemical stabilities, enabling them

* Corresponding authors at: Oxide & Organic Nanomaterials for Energy & Environment (ONE) Laboratory, Physical Science & Engineering (PSE), King Abdullah University of Science and Technology (KAUST), Thuwal 23955, Saudi Arabia.
E-mail addresses: javeed.mahmood@kaust.edu.sa (J. Mahmood), cafer.yavuz@kaust.edu.sa (C.T. Yavuz).

https://doi.org/10.1016/j.cej.2023.142474
Received 1 December 2022; Received in revised form 6 March 2023; Accepted 15 March 2023
Available online 18 March 2023

to survive extremely harsh conditions.

In this work, we designed a sintering-resistant catalyst by anchoring metal nanoparticles on the vertically standing 2D (V2D) fused aromatic ladder polymers for low temperature catalytic ammonia decomposition. Ammonia is an emerging green hydrogen carrier with high-capacity delivery potential (121 kg H_2/m^3, 17.64 wt% of H_2 capacity) [23] and its low temperature cracking is an outstanding industrial challenge for the safe transport of hydrogen. Since ruthenium (Ru) metal shows optimum binding energy with ammonia, it is frequently selected as the active metal for catalytic ammonia cracking [23–25]. When we loaded a similar amount of Ru onto the 2D carbon structures, the V2D support prevented the aggregation of metal particles, resulting in a smaller particle size and uniform distribution than a planar 2D (P2D) framework. The Ru-V2D showed a significantly higher ammonia conversion rate at a high gas hourly space velocity (GHSV). Our results unlock the potential of carefully designed support geometries for outstanding catalytic activities and kinetics.

2. Results and discussion

We prepared two polymer network structures with pore sizes as similar as possible to reduce the difference in the structural parameters (Fig. 1) to study the 2D support effects. The conventional planar 2D (P2D) structure was prepared by combining triphenylene-2,3,6,7,10,11-hexamine (TPHA) hexahydrochloride with pyrene-4,5,9,10-tetraone (tetraketopyrene, TKP), and the vertically standing 2D (V2D) structure was synthesized by triptycene hexamine (THA) instead of TPHA (see the section on experimental procedures in the Supplementary Information). The rigid synchronous formation of phenazine rings provides directionality to the extended structure and facilitates the 2D growth of the ladder-type backbone [26]. During the reaction, $RuCl_3$ serves as a Lewis acid to catalyze pyrazine synthesis, and the formation of fused aromatic phenazine linkages provide a robust framework with excellent thermal stability. In addition, the pyrazine interacts with Ru cations to stably anchor the metal, thereby helping to form nanoparticles during subsequent reduction and thermal treatments, and eliminating the separate deposition [3]. After annealing the samples at 800 °C, Ru-V2D showed a larger visual sample volume than Ru-P2D (Fig. S1) because its perpendicular growth gives a loosened packed structure and is expected to have good gas permeability [27–29].

To avoid compositional differences stemming from experimental conditions, heat-treated Ru-V2D, Ru-P2D, and Ru/C (commercial) were all prepared to have similar amounts of Ru. In an effort to select the best Ru quantification method, we reviewed the literature and found that three methods are often employed: (1) assuming the mixing ratio from the synthesis procedure to remain the same in the final structure [30–32], (2) using inductively coupled plasma-optical emission spectroscopy (ICP-OES) [33], or (3) X-ray fluorescence (XRF) elemental ratios (Table S1) [34]. However, each of these three methods has severe limitations. When mixing ratios are considered, it generally assumes that the carbon, hydrogen, and nitrogen content of the composite materials stay unchanged after the heat treatment. The Ru percentage, however, almost always increases in the actual tested sample as the organic components decompose by heat treatment-induced pyrolysis. The solubility of Ru is often too poor to be precisely measured by ICP-OES (requires a large amount of solvent or else leads to underestimation) [35], and the XRF is a highly sensitive surface analysis tool that gives a rough estimate of the surface cross sections for most of the trace elements [36,37]. Therefore, we decided to minimize the uncertainty of the Ru content and found that the residue of thermogravimetric analysis (TGA) in the air gives the most accurate value for the Ru content (Fig. S2 and S3). The Ru content of each catalyst was, therefore, confirmed as 12.42 (Ru-V2D), 13.24 (Ru-P2D), and 12.08 wt% (Ru/C).

The structural analysis was carried out to observe the differences between the two newly developed catalysts. The N_2 adsorption isotherms (based on Brunauer-Emmett-Teller (BET) theory) and pore size

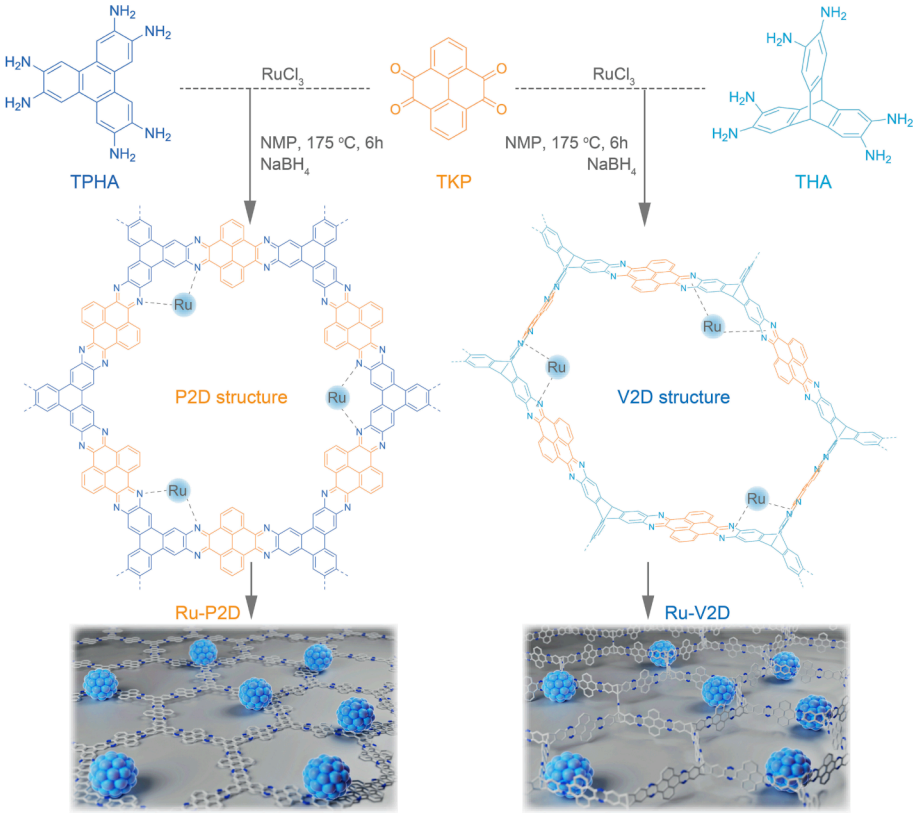

Fig. 1. Synthesis of the Ru-anchored planar 2D (Ru-P2D) and vertically standing 2D (Ru-V2D) structures (cyan ball: Ru particle, gray: carbon, blue: nitrogen). (For interpretation of the references to colour in this figure legend, the reader is referred to the web version of this article.)

distributions (from Non-Local Density Functional Theory – NLDFT) of Ru loaded 2D frameworks show similar profiles as before the metal loading, which is prepared by trifluoromethanesulfonic acid (TFMSA) [20]. The Ru-V2D has a high surface area of over 1100 $m^2 g^{-1}$ even after metal nanoparticle anchoring (Fig. 2A) [20]. The specific surface area of Ru-V2D (1130 $m^2 g^{-1}$) is almost twice that of the Ru-P2D, which is only 627 $m^2 g^{-1}$. The pore size distribution from the NLDFT shows 0.7 nm, similar to pristine structures (Fig. 2A inset). In the case of commercial Ru/C, it has 840 $m^2 g^{-1}$ with 0.49 nm of main pore width (Fig. S4). Interestingly, the Ru cations are also reduced to Ru^0 as particles form, even though the thermal treatment is carried out at just 800 °C.

The powder X-ray diffraction (XRD) patterns show carbonized supports with embedded Ru nanoparticles (Fig. 2B, Fig. S4). In the case of Ru-P2D, the polymeric structures carbonize during the heat treatment and increase the π-π interactions between the layers to form bigger Ru nanoparticles through limited penetration between the layers. In contrast, the nanoparticles of Ru-V2D did not grow as much like in the Ru-P2D, even though it contains a similar amount of Ru. The particle size distributions from transmission electron microscopy (TEM) (Fig. 2C) revealed that the Ru-V2D has an average particle size of 2.3 nm, less than half of the Ru-P2D (5.3 nm). This trend is consistent with the powder XRD results calculated from the Scherrer equation as 1.72 nm and 4.81 nm, respectively. It is highly probable that in Ru-P2D, Ru moves over a conventional layered structure during heat treatment and forms larger particles due to aggregation, consistent with *Hüttig* temperature [19]. On the other hand in Ru-V2D, vertically standing pyrazine N anchors the Ru particles and blocks the path of aggregation, preventing further particle growth. The 600 °C treated Ru/C showed irregular particle size distribution because of their broad range of carbon structural morphology (Fig. S4).

The bonding nature of the catalysts was analyzed by X-ray photoelectron spectroscopy (XPS) (Fig. 3A). The formation of the pyrazine ring is confirmed by the C1s peak centered at 285.84 eV and N1s at 397.98 eV. The appearance of Ru nanoparticles after the heat treatment was verified from the peak at 280.34 eV for Ru^0. As carbonization proceeds, the percentage of pyridine N is reduced, and pyrrolic N

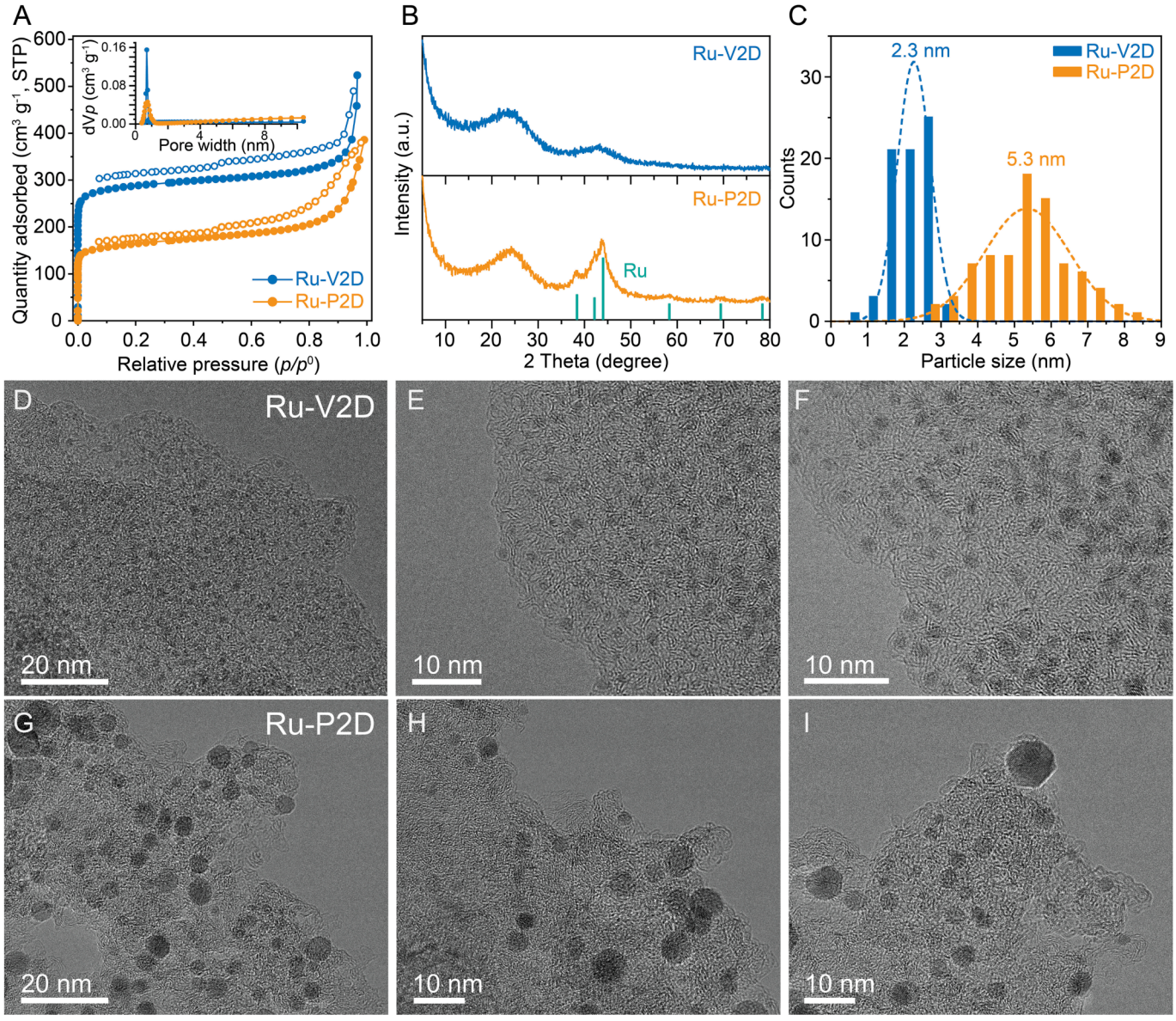

Fig. 2. Structural investigation of Ru-anchored V2D (Ru-V2D) and P2D (Ru-P2D) networks. (A) Nitrogen adsorption/desorption isotherms at 77 K. Inset: NLDFT pore size distribution. (B) X-ray diffraction patterns (XRD) of two structures with Ru peaks (PDF no. 89–4903, cyan bar), (C) Histograms of the particle size distribution for fresh Ru nanoparticles. TEM images of Ru-V2D (D-F) and Ru-P2D (G-I). (For interpretation of the references to colour in this figure legend, the reader is referred to the web version of this article.)

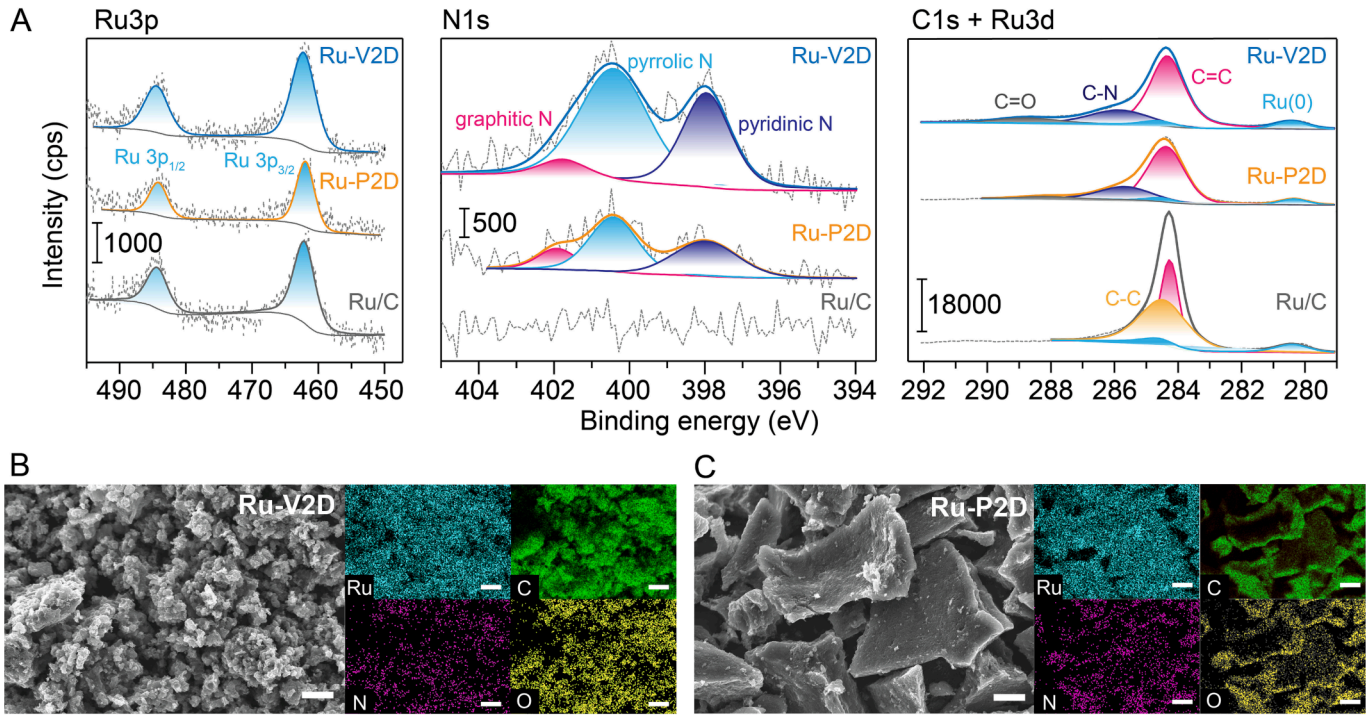

Fig. 3. Elemental mapping and electron microscopic analysis for Ru catalysts. (A) X-ray photoelectron spectroscopy (XPS) spectra of Ru-V2D, Ru-P2D, and Ru/C. The graphs for Ru3p, N1s, and C1s + Ru3d are shown. (B) Scanning electron microscopy images of Ru-V2D and (C) Ru-P2D with Energy-dispersive X-ray spectroscopy (EDS) mapping of the catalysts (scale bar: 10 mm).

(400.55 eV) along with graphitic N (401.82 eV) increases. The flat P2D structure undergoes carbonization more quickly with lower N1s intensity than V2D. The heat-treated Ru/C follows the same tendency. The scanning electron microscopy (SEM) image analysis shows that Ru-V2D has powder-like morphology (Fig. 3B), and Ru-P2D has layer-type morphology (Fig. 3C). The elemental composition and the distribution are confirmed by the energy-dispersive X-ray spectroscopy (EDS) mapping.

The decomposition of ammonia ($2NH_3$ (g) → N_2 (g) + $3H_2$ (g)) is an endothermic reaction (ΔH^0) of + 42 kJ mol^{-1} at standard temperature and pressure (STP); it requires an energy input to overcome the activation energy barrier. Therefore, developing efficient catalysts that can lower this barrier is crucial. Various factors, such as the particle size of the catalyst metal and the nature of the catalyst support, influence the catalytic activity of ammonia decomposition. Carbon-based materials have emerged as promising candidates for catalytic support due to their electron-rich and conductive nature and strong basicity, which can enhance the catalytic efficiency of the system. Specifically, it has been reported that electron-rich, conductive support materials with strong basicity exhibit high catalytic efficiency [38]. Therefore, carbon-based materials are considered suitable and durable catalytic supports for ammonia cracking reactions.

To investigate the role of support structure on the catalytic activity, the NH_3 cracking performance of Ru-V2D, Ru-P2D, and commercial Ru/C (Ru on activated carbon) were tested in the same conditions. To prepare all the catalysts for ammonia decomposition, experiments were typically carried out at 350–550 °C; Ru/C was also heat-treated at 600 °C under inert conditions. The catalytic activities of all catalysts were evaluated simultaneously using a four-channel reactor system to reduce experimental and user errors. In addition, samples having similar amounts of Ru were prepared to minimize the differences in performance due to the amounts of Ru.

For the fast H_2 production from NH_3, it is essential to show a high conversion rate at a high GHSV [23,39–41]. Therefore, the mass of catalysts was kept constant while the flow rate varied, and the conversion rates were actively monitored (Fig. 4A) by a gas chromatogram (GC). As the GHSV value increased from 5,500 to 32,000 mL g_{cat}^{-1} h^{-1}, the NH_3 conversion decreased for all catalysts, as expected. The Ru-V2D catalyst shows hydrogen generation performance at least twice more than the Ru-P2D and Ru/C catalysts (Fig. 4B) and highly competitive activity compared to reported catalysts (Table S1) with higher TOF (Fig. S5). The activation energy was calculated using the Arrhenius equation at a lower conversion region, showing that Ru-V2D had 82.43 kJ mol^{-1}, Ru-P2D had 82.75 kJ mol^{-1}, and Ru/C had 91.94 kJ mol^{-1} (Fig. S6).

There are two main reasons why Ru-V2D shows high performance. First, Ru-V2D has a smaller particle size distribution than Ru-P2D, providing more active sites. This is predominantly because the aggregation opportunity is less in a vertically standing (V2D) structure than that of a flat (P2D) one. Secondly, the sp^2 orbitals perpendicular to the growth plane are difficult to interact with other planes, expanding the surface area and allowing more gas molecules to penetrate and react quickly. Therefore, on the vertically standing 2D structures, the active metal particles are distributed uniformly, enabling them to be efficiently utilized even at a fast gas flow rate.

In a continuous temperature ramping experiment, Ru-V2D and Ru-P2D were heated to 350–500 °C and back (Fig. S7). Interestingly, when the ammonia decomposition temperature was reverted back to 450 °C after testing at 500 °C, the Ru-V2D catalyst maintained its catalytic activity the same as before the heating, while in the case of Ru-P2D, the activity decreased. After the reaction, the catalysts were collected to investigate the morphology changes in the catalyst by TEM analysis. The TEM images indicated that Ru nanoparticles preserved their size in the Ru-V2D catalyst with no apparent changes in the morphology (Fig. 4D). On the other hand, the particles grew bigger in the case of Ru-P2D and Ru/C after the catalytic reaction (Fig. 4E, Fig. S4). The average particle size distribution of Ru-P2D changed from 5 to 10 nm, with no particular growth pattern. In the case of the commercial Ru/C, it exhibited a bigger particle size (50 nm) in a wider size distribution (Fig. S4). The generated hydrogen gas may lead to

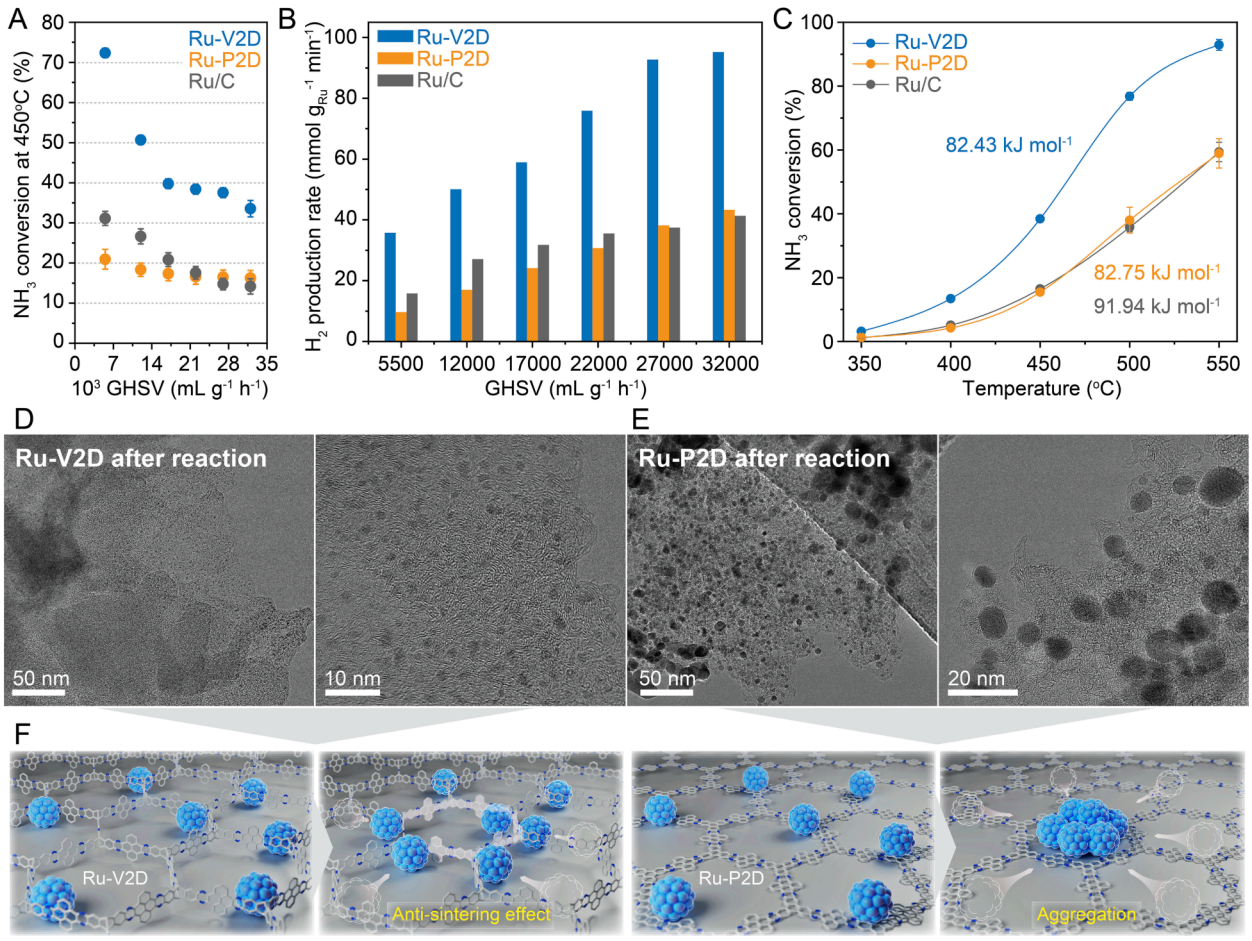

Fig. 4. Ammonia decomposition study under practical gas flow and reaction temperatures. (A) Ammonia decomposition conversion graph at 450 °C according to flow rates. (B) Hydrogen production rate per Ru contents (mmol g_{Ru}^{-1} h^{-1}) at 450 °C in each structure. (C) Decomposition conversion curves and activation energy of each structure at $P = 1$ atm; $T = 350$–550 °C, GHSV: 22,000 mL g_{cat}^{-1} h^{-1}. (D, E) TEM images of Ru-V2D (D) and Ru-P2D (E) after ammonia decomposition reaction. (F) Illustration of the anti-sintering effect of the V2D vs. P2D structure.

aggregation by promoting reductive mobility on the Ru particles during ammonia decomposition [42]. However, the V2D structure showed aggregation blocking by vertical carbon obstructions prevented such unwanted growth, providing long-term stable activity. The Ru-V2D showed stable activity and unchanging structure even after 10 cycles of the NH_3 decomposition test (150 h, Fig. S8). Combining ammonia decomposition and structural analysis from the tested catalysts, we concluded that vertically grown 2D structures promote catalytic activity by particle size control and provide catalytic stability by preventing further aggregation (Fig. 4F).

3. Conclusions

In conclusion, we have shown the effect of vertical obstruction for particle size control in Ru nanoparticle-loaded 2D porous pyrazine frameworks. Ammonia cracking was selected as an industrially promising reaction to study the impact of the support design. The planar 2D carbons led to undesirable aggregation in Ru nanoparticles, lowering the catalytic activity over long reaction times. The vertically standing frameworks provided stoppers for aggregation prevention, resulting in enhanced activity and longevity in ammonia cracking. The findings show the need for geometric modification of support frameworks for containing and guiding active metal sites for enhanced catalytic activities.

Declaration of Competing Interest

The authors declare that they have no known competing financial interests or personal relationships that could have appeared to influence the work reported in this paper.

Data availability

Data will be made available on request.

Acknowledgements

This research was supported by the King Abdullah University of Science and Technology (KAUST), Kingdom of Saudi Arabia, and the Nurturing Next-generation Researchers (2021R1A6A3A03039501) from the National Research Foundation (NRF) of Korea, Republic of Korea. The authors thank Ivan Gromicho of KAUST for the illustrations used in Figs. 1 and 4.

Appendix A. Supplementary data

Supplementary data to this article can be found online at https://doi.org/10.1016/j.cej.2023.142474.

References

[1] J. Mahmood, M.A.R. Anjum, J.B. Baek, Fused Aromatic Network Structures as a Platform for Efficient Electrocatalysis, Adv. Mater. 31 (20) (2019) 1805062.

[2] Y. Song, E. Ozdemir, S. Ramesh, A. Adishev, S. Subramanian, A. Harale, M. Albuali, B.A. Fadhel, A. Jamal, D. Moon, S.H. Choi, C.T. Yavuz, Dry reforming of methane by stable Ni-Mo nanocatalysts on single-crystalline MgO, Science 367 (6479) (2020) 777–781.

[3] Y.Z. Yu, Y.M. Gan, C.Q. Huang, Z.H. Lu, Z.E.W. Wang, R.B. Zhang, G. Feng, Ni/La_2O_3 and Ni/MgO-La_2O_3 catalysts for the decomposition of NH_3 into hydrogen, Int J Hydrog. Energy 45 (33) (2020) 16528–16539.

[4] C. Huang, H. Li, J. Yang, C. Wang, F. Hu, X. Wang, Z.-H. Lu, G. Feng, R. Zhang, $Ce_{0.6}Zr_{0.3}Y_{0.1}O_2$ solid solutions-supported NiCo bimetal nanocatalysts for NH_3 decomposition, Appl. Surf. Sci. 478 (2019) 708–716.

[5] J. Mahmood, F. Li, S.M. Jung, M.S. Okyay, I. Ahmad, S.J. Kim, N. Park, H.Y. Jeong, J.B. Baek, An efficient and pH-universal ruthenium-based catalyst for the hydrogen evolution reaction, Nat. Nanotechnol. 12 (5) (2017) 441–446.

[6] J. Kim, O. Gwon, O. Kwon, J. Mahmood, C. Kim, Y. Yang, H. Lee, J.H. Lee, H. Y. Jeong, J.B. Baek, G. Kim, Synergistic Coupling Derived Cobalt Oxide with Nitrogenated Holey Two-Dimensional Matrix as an Efficient Bifunctional Catalyst for Metal-Air Batteries, ACS Nano 13 (5) (2019) 5502–5512.

[7] S.J. Kim, J. Mahmood, C. Kim, G.F. Han, S.W. Kim, S.M. Jung, G.M. Zhu, J.J. De Yoreo, G. Kim, J.B. Baek, Defect-Free Encapsulation of Fe^0 in 2D Fused Organic Networks as a Durable Oxygen Reduction Electrocatalyst, J. Am. Chem. Soc. 140 (5) (2018) 1737–1742.

[8] Y. Shao, Z.T. Zha, H. Wang, Heteroatom-doped porous carbon-supported single-atom catalysts for electrocatalytic energy conversion, J. Energy Chem. 63 (2021) 54–73.

[9] M. Bosilj, L. Rustam, R. Thomann, J. Melke, A. Fischer, R.J. White, Directing nitrogen-doped carbon support chemistry for improved aqueous phase hydrogenation catalysis, Cat. Sci. Technol. 10 (14) (2020) 4794–4808.

[10] A. Riano, K. Strutynski, M. Liu, C.T. Stoppiello, B. Lerma-Berlanga, A. Saeki, C. Marti-Gastaldo, A.N. Khlobystov, G. Valenti, F. Paolucci, M. Melle-Franco, A. Mateo-Alonso, An Expanded 2D Fused Aromatic Network with 90-Ring Hexagons, Angew. Chem. Int. Ed. 61 (2) (2022) e202113657.

[11] J. Zhu, S. Wu, X. Hou, J. Wu, 1,6-Anthrazoline-Linked pi-Conjugated Macrocycles and Two-Dimensional Polymer via Friedlander Synthesis, Angew. Chem. Int. Ed. 60 (48) (2021) 25323–25327.

[12] M. Wang, M. Ballabio, M. Wang, H.H. Lin, B.P. Biswal, X. Han, S. Paasch, E. Brunner, P. Liu, M. Chen, M. Bonn, T. Heine, S. Zhou, E. Canovas, R. Dong, X. Feng, Unveiling Electronic Properties in Metal-Phthalocyanine-Based Pyrazine-Linked Conjugated Two-Dimensional Covalent Organic Frameworks, J. Am. Chem. Soc. 141 (42) (2019) 16810–16816.

[13] S. Che, L. Fang, Porous Ladder Polymer Networks, Chem 6 (10) (2020) 2558–2590.

[14] J.T. Xu, J. Mahmood, Y.H. Dou, S.X. Dou, F. Li, L.M. Dai, J.B. Baek, 2D Frameworks of C_2N and C_3N as New Anode Materials for Lithium-Ion Batteries, Adv. Mater. 29 (34) (2017) 1702007.

[15] S.Y. Yu, J. Mahmood, H.J. Noh, J.M. Seo, S.M. Jung, S.H. Shin, Y.K. Im, I.Y. Jeon, J. B. Baek, Direct Synthesis of a Covalent Triazine-Based Framework from Aromatic Amides, Angew. Chem. Int. Ed. 57 (28) (2018) 8438–8442.

[16] J. Mahmood, M.A.R. Anjum, S.H. Shin, I. Ahmad, H.J. Noh, S.J. Kim, H.Y. Jeong, J. S. Lee, J.B. Baek, Encapsulating Iridium Nanoparticles Inside a 3D Cage-Like Organic Network as an Efficient and Durable Catalyst for the Hydrogen Evolution Reaction, Adv. Mater. 30 (52) (2018) 1805606.

[17] X.L. Li, C.L. Zhang, S.L. Cai, X.H. Lei, V. Altoe, F. Hong, J.J. Urban, J. Ciston, E. M. Chan, Y. Liu, Facile transformation of imine covalent organic frameworks into ultrastable crystalline porous aromatic frameworks, Nat. Commun. 9 (2018) 2998.

[18] C.K. Jin, L.H. Cheng, G. Feng, R.P. Ye, Z.H. Lu, R.B. Zhang, X.H. Yu, Adsorption of Transition-Metal Clusters on Graphene and N-Doped Graphene: A DFT Study, Langmuir 38 (12) (2022) 3694–3710.

[19] Y.Q. Dai, P. Lu, Z.M. Cao, C.T. Campbell, Y.N. Xia, The physical chemistry and materials science behind sinter-resistant catalysts, Chem. Soc. Rev. 47 (12) (2018) 4314–4331.

[20] S.J. Kim, T.H. Kim, I. Ahmad, H.J. Noh, S.M. Jung, Y.K. Im, J. Mahmood, Y.S. Bae, J.B. Baek, Fused aromatic networks with the different spatial arrangement of structural units, Cell. Rep. Phys. Sci. 2 (7) (2021), 100502.

[21] H.J. Noh, Y.K. Im, S.Y. Yu, J.M. Seo, J. Mahmood, T. Yildirim, J.B. Baek, Vertical two-dimensional layered fused aromatic ladder structure, Nat. Commun. 11 (1) (2020) 2021.

[22] I. Rose, C.G. Bezzu, M. Carta, B. Comesana-Gandara, E. Lasseuguette, M.C. Ferrari, P. Bernardo, G. Clarizia, A. Fuoco, J.C. Jansen, K.E. Hart, T.P. Liyana-Arachchi, C. M. Colina, N.B. McKeown, Polymer ultrapermeability from the inefficient packing of 2D chains, Nat. Mater. 16 (9) (2017) 932–937.

[23] S. Mukherjee, S.V. Devaguptapu, A. Sviripa, C.R.F. Lund, G. Wu, Low-temperature ammonia decomposition catalysts for hydrogen generation, Appl. Catal. B Environ. 226 (2018) 162–181.

[24] C.Q. Chen, K. Wu, H.J. Ren, C. Zhou, Y. Luo, L. Lin, C.T. Au, L.L. Jiang, Ru-Based Catalysts for Ammonia Decomposition: A Mini-Review, Energ. Fuel 35 (15) (2021) 11693–11706.

[25] K. McCullough, P.H. Chiang, J.D. Jimenez, J.A. Lauterbach, Material Discovery and High Throughput Exploration of Ru Based Catalysts for Low Temperature Ammonia Decomposition, Materials 13 (8) (2020) 1869.

[26] B. Zhang, M.F. Wei, H.Y. Mao, X.K. Pei, S.A. Alshmimri, J.A. Reimer, O.M. Yaghi, Crystalline Dioxin-Linked Covalent Organic Frameworks from Irreversible Reactions, J. Am. Chem. Soc. 140 (40) (2018) 12715–12719.

[27] B.S. Ghanem, M. Hashem, K.D.M. Harris, K.J. Msayib, M.C. Xu, P.M. Budd, N. Chaukura, D. Book, S. Tedds, A. Walton, N.B. McKeown, Triptycene-Based Polymers of Intrinsic Microporosity: Organic Materials That Can Be Tailored for Gas Adsorption, Macromolecules 43 (12) (2010) 5287–5294.

[28] B.S. Ghanem, K.J. Msayib, N.B. McKeown, K.D.M. Harris, Z. Pan, P.M. Budd, A. Butler, J. Selbie, D. Book, A. Walton, A triptycene-based polymer of intrinsic microposity that displays enhanced surface area and hydrogen adsorption, Chem. Commun. 1 (2007) 67–69.

[29] B.S. Ghanem, R. Swaidan, E. Litwiller, I. Pinnau, Ultra-Microporous Triptycene-based Polyimide Membranes for High-Performance Gas Separation, Adv. Mater. 26 (22) (2014) 3688–3692.

[30] Z.Q. Wang, Y.M. Qu, X.L. Shen, Z.F. Cai, Ruthenium catalyst supported on Ba modified ZrO_2 for ammonia decomposition to COx-free hydrogen, Int. J. Hydrog. Energy 44 (14) (2019) 7300–7307.

[31] Z.Q. Wang, Z.F. Cai, Z. Wei, Highly Active Ruthenium Catalyst Supported on Barium Hexaaluminate for Ammonia Decomposition to COx-Free Hydrogen, ACS Sustain. Chem. Eng. 7 (9) (2019) 8226–8235.

[32] C.Q. Huang, Y.Z. Yu, J.M. Yang, Y. Yan, D.S. Wang, F.Y. Hu, X.W. Wang, R. B. Zhang, G. Feng, Ru/La_2O_3 catalyst for ammonia decomposition to hydrogen, Appl. Surf. Sci. 476 (2019) 928–936.

[33] S. Sayas, N. Morlanes, S.P. Katikaneni, A. Harale, B. Solami, J. Gascon, High pressure ammonia decomposition on Ru-K/CaO catalysts, Cat. Sci. Technol. 10 (15) (2020) 5027–5035.

[34] S.J. Wang, S.F. Yin, L. Li, B.Q. Xu, C.F. Ng, C.T. Au, Investigation on modification of Ru/CNTs catalyst for the generation of COx-free hydrogen from ammonia, Appl. Catal. B Environ. 52 (4) (2004) 287–299.

[35] M. Balcerzak, Analytical methods for the determination of ruthenium: The state of the art, Crit. Rev. Anal. Chem. 32 (3) (2002) 181–226.

[36] J.Q. McComb, C. Rogers, F.X.X. Han, P.B. Tchounwou, Rapid Screening of Heavy Metals and Trace Elements in Environmental Samples Using Portable X-Ray Fluorescence Spectrometer, A Comparative Study, Water Air Soil Poll. 225 (12) (2014).

[37] J.B. Gilbert, M.F. Rubner, R.E. Cohen, Depth-profiling X-ray photoelectron spectroscopy (XPS) analysis of interlayer diffusion in polyelectrolyte multilayers, Proc. Natl. Acad. Sci. U.S.A. 110 (17) (2013) 6651–6656.

[38] X.Y. Lu, A. Roldan, Are Carbon-Based Materials Good Supports for the Catalytic Reforming of Ammonia? J. Phys. Chem. C 125 (29) (2021) 15950–15958.

[39] F. Schuth, R. Palkovits, R. Schlogl, D.S. Su, Ammonia as a possible element in an energy infrastructure: catalysts for ammonia decomposition, Energ. Environ. Sci. 5 (4) (2012) 6278–6289.

[40] F.B. Juangsa, A.R. Irhamna, M. Aziz, Production of ammonia as potential hydrogen carrier: Review on thermochemical and electrochemical processes, Int. J. Hydrog. Energy 46 (27) (2021) 14455–14477.

[41] J. Cha, Y.S. Jo, H. Jeong, J. Han, S.W. Nam, K.H. Song, C.W. Yoon, Ammonia as an efficient COx-free hydrogen carrier: Fundamentals and feasibility analyses for fuel cell applications, Appl. Energ. 224 (2018) 194–204.

[42] P.K. Babu, H.S. Kim, S.T. Kuk, J.H. Chung, E. Oldfield, A. Wieckowski, E. S. Smotkin, Activation of nanoparticle Pt-Ru fuel cell catalysts by heat treatment: A ^{195}Pt NMR and electrochemical study, J. Phys. Chem. B 109 (36) (2005) 17192–17196.